



Chronic lymphocytic leukemia

# Distinct roles for phosphoinositide 3-kinases $\gamma$ and $\delta$ in malignant B cell migration

Ahmed Y. Ali<sup>1,2</sup> · Xun Wu<sup>1</sup> · Nour Eissa<sup>1</sup> · Sen Hou<sup>1</sup> · Jean-Eric Ghia<sup>1,3</sup> · Thomas T. Murooka<sup>1,4</sup> · Versha Banerji<sup>2,5</sup> · James B. Johnston<sup>2</sup> · Francis Lin<sup>1,6</sup> · Spencer B. Gibson<sup>1,2,5</sup> · Aaron J. Marshall<sup>1,2,5</sup>

Received: 18 August 2017 / Revised: 13 December 2017 / Accepted: 15 December 2017 / Published online: 31 January 2018  
© The Author(s) 2018. This article is published with open access

## Abstract

The PI 3-kinases (PI3K) are essential mediators of chemokine receptor signaling necessary for migration of chronic lymphocytic leukemia (CLL) cells and their interaction with tissue-resident stromal cells. While the PI3K $\delta$ -specific inhibitor idelalisib shows efficacy in treatment of CLL and other B cell malignancies, the function of PI3K $\gamma$  has not been extensively studied in B cells. Here, we assess whether PI3K $\gamma$  has non-redundant functions in CLL migration and adhesion to stromal cells. We observed that pharmaceutical PI3K $\gamma$  inhibition with CZC24832 significantly impaired CLL cell migration, while dual PI3K $\delta/\gamma$  inhibitor duvelisib had a greater impact than single isoform-selective inhibitors. Knockdown of PI3K $\gamma$  reduced migration of CLL cells and cell lines. Expression of the PI3K $\gamma$  subunits increased in CLL cells in response to CD40L/IL-4, whereas BCR cross-linking had no effect. Overexpression of PI3K $\gamma$  subunits enhanced cell migration in response to SDF1 $\alpha$ /CXCL12, with the strongest effect observed within ZAP70 + CLL samples. Microscopic tracking of cell migration within chemokine gradients revealed that PI3K $\gamma$  functions in gradient sensing and impacts cell morphology and F-actin polarization. PI3K $\gamma$  inhibition also reduced CLL adhesion to stromal cells to a similar extent as idelalisib. These findings provide the first evidence that PI3K $\gamma$  has unique functions in malignant B cells.

**Electronic supplementary material** The online version of this article (<https://doi.org/10.1038/s41375-018-0012-5>) contains supplementary material, which is available to authorized users.

✉ Aaron J. Marshall  
aaron.marshall@umanitoba.ca

- <sup>1</sup> Department of Immunology, University of Manitoba, 750 McDermot Avenue, Winnipeg, MB R3E 0T5, Canada
- <sup>2</sup> Research Institute in Oncology and Hematology, CancerCare Manitoba, 675 McDermot Ave., Winnipeg, MB R3E 0V9, Canada
- <sup>3</sup> Department of Internal Medicine, Section of Gastroenterology, University of Manitoba, 820 Sherbrooke St., Winnipeg, MB R3A 1R9, Canada
- <sup>4</sup> Department of Medical Microbiology and Infectious Diseases, University of Manitoba, 745 Bannatyne Ave., Winnipeg, MB R3E 0J9, Canada
- <sup>5</sup> Department of Biochemistry and Medical Genetics, University of Manitoba, 745 Bannatyne Ave., Winnipeg, MB R3E 0J9, Canada
- <sup>6</sup> Department of Physics and Astronomy, University of Manitoba, Allen Building, Winnipeg, MB R3T 2N2, Canada

## Introduction

Chronic lymphocytic leukemia (CLL) is a prevalent hematologic malignancy affecting adults in the West. CLL cells rely on chronic activation triggered via the B cell receptor (BCR) to potentiate their survival [1]. Within lymphoid tissues, CLL cells interact with and shape a microenvironment favorable to their survival and proliferation [2]. They migrate to favorable niches in response to chemotactic factors, such as the chemokine stromal-derived factor 1 (SDF1 $\alpha$ ). They interact with resident stromal cells that provide them with survival and proliferative stimuli through cell–cell contact and soluble factors [3–5]. The protective microenvironment shields CLL cells from the effects of therapeutics, conferring a resistant phenotype.

CLL varies from indolent to progressive forms according to the expression of several biomarkers, immunoglobulin variable heavy chain (IgVH) mutation, and chromosomal abnormalities [6, 7]. One such biomarker is the expression of zeta-chain T cell receptor-associated protein kinase 70 kDa (ZAP70) [8, 9]. We and others have shown that ZAP70 expression can alter CLL adhesion and migration [10–12]; however, the mechanisms for this remain unclear.

The phosphoinositide 3-kinase (PI3K) signaling pathway has been implicated in numerous malignancies [13–17]. PI3K enzymes phosphorylate the 3' hydroxyl group of the inositol ring of phosphoinositide lipids. PI3K $\delta$  has established functions in normal and malignant B cell signaling, and the p110 $\delta$ -specific inhibitor idelalisib has been effective in CLL treatment [18, 19]. Inhibition of PI3K $\delta$  affects multiple aspects of CLL biology, including cell adhesion and migration in response to chemokines [20, 21].

PI3K $\gamma$  consists of a catalytic subunit (p110 $\gamma$ ) and one of two regulatory subunits (p84 or p101), which bind to p110 $\gamma$  and have different effects on p110 $\gamma$  activity in terms of cellular migration [22, 23]. PI3K $\gamma$  is recruited to activated chemokine receptors via p101-dependent binding to G $\beta$ / $\gamma$  subunits [24–26], whereas the mechanism of PI3K $\delta$  activation by chemokines is unclear. PI3K $\gamma$  has well-established functions in T lymphocyte and neutrophil chemokine receptor signaling, but has not been extensively studied in B lymphocytes [27, 28]. In fact, the limited data available on B cell function in PI3K $\gamma$ -deficient mice indicate that this enzyme is not essential for B cell activation or migration [29, 30]. Despite this, PI3K $\gamma$  inhibitors are now in clinical development for B cell malignancies [31].

In this study, we present our novel findings that PI3K $\delta$  and PI3K $\gamma$  have unique, non-redundant functions in CLL cell migration and adhesion to stromal cells. These findings indicate that targeting PI3K $\gamma$  alone or in combination with PI3K $\delta$  may have a unique impact on CLL biology with potential therapeutic benefit.

## Materials and methods

### CLL cells and cell lines

CLL cells were isolated from peripheral blood samples using RosetteSep Human B Cell Enrichment Cocktail (Stemcell Technologies) at CancerCare Manitoba with the approval of the Research Ethics Board at the University of Manitoba. ZAP70 and IgVH mutation status were determined as previously described [32]. Patient characteristics are described in Table S1. CLL-derived JVM3 and Burkitt lymphoma Ramos cells were obtained from DSMZ, Germany. HS-5 human bone marrow-derived stromal cells were obtained from ATCC. All cells were grown in RPMI1640 media supplemented with 10% fetal bovine serum and 1% penicillin-streptomycin (GIBCO).

### Chemicals and reagents

PI3K inhibitors CZC24832, GS-1101/idelalisib, IPI-145/duvelisib, and GDC-0980/apitolisib (Selleck Chemicals)

were reconstituted in DMSO (Sigma) and used at final concentrations of 2  $\mu$ M (CZC24832) and 1  $\mu$ M (idelalisib, duvelisib, GDC-0980). CZC24832 has greater than 10-fold selectivity over PI3K $\beta$  and greater than 100-fold selectivity over PI3K $\alpha$  and PI3K $\delta$  [33].  $\alpha$ -IgM F(ab')<sub>2</sub> (Southern Biotech) was used at 10  $\mu$ g/ml and CD40 ligand and interleukin 4 (R&D systems) were used at 50 ng/ml each. Anti-p110 $\gamma$  antibody, anti-Akt antibody, anti-pAkt Ser473 antibody, anti-GAPDH antibody (Cell Signaling), anti-p101 antibody (R&D systems), and Mini-PROTEAN TGX pre-cast gels (Bio-Rad) were used for Western blot analysis. SDF1 $\alpha$  (Peprotech) was used at 100 ng/ml. Alexa Fluor<sup>®</sup> 488 Phalloidin (Life Technologies) was used at 33 nM for F-actin staining. Superscript VILO cDNA mix (Invitrogen) was used for RT-qPCR. DAPI, trypsin-EDTA (Sigma), and anti CD19-FITC antibody (BD Biosciences) were used for the cell adhesion assay.

### Western blotting

The experiments were performed as previously described [34]. Membranes were incubated overnight at 4 °C with anti-p110 $\gamma$  and anti-p101 antibodies (1:1000 dilution). GAPDH served as a loading control (1:10,000 dilution). HRP-conjugated anti-rabbit (Cell Signaling) and anti-mouse (Jackson Immunoresearch) secondary antibodies (1:5000 dilution) were used for chemiluminescent detection.

### Real-time quantitative PCR

The experiments were performed as previously described [35]. Briefly, 5 million CLL cells per treatment group were stimulated for 24 h with  $\alpha$ -IgM or CD40L/IL-4, collected in TRIzol, and total RNA was isolated and purified using the Purelink RNA kit (Thermo Fisher). qPCR was performed using a LightCycler 96 PCR instrument (Roche Diagnostics) and Power SYBR green (Applied Biosystems). All reactions were run in duplicates (primer sequences available in Fig. S1A).

### Plasmid constructs

Expression vectors for p110 $\gamma$ -GFP or p101-GFP used the pLenti-GIII-CMV-GFP-2A-Puro backbone (Applied Biological Materials). The expression vector for dCas9-GFP is pLV-hUbc-dCas9-T2A-GFP (Addgene #53191). Guide RNA expression cassettes targeting the p110 $\gamma$  gene were designed based on a CRISPRi optimized gRNA sequence library [36] and synthesized by Integrated DNA Technologies (sequences in Fig. S1B). gRNA cassettes were cloned into the XbaI/XhoI sites of vector pU6-sgRNA EF1Alpha-puro-T2A-BFP (Addgene #60955) for use in CRISPRi (Fig. S1B). For CRISPRi experiments, the two p110 $\gamma$

gRNA plasmid vectors were mixed with dCas9-GFP plasmid at a 3:1 ratio (gRNA:dCas9) for transfection.

## Cell transfection

For cell lines,  $5 \times 10^5$  cells were transfected with each plasmid (1  $\mu$ g) using the Neon Transfection system (Invitrogen), with the following conditions: JVM3 1200 V, 20 ms, 2 pulses; Ramos 1600 V, 20 ms, 1 pulse. For primary CLL cells,  $1 \times 10^6$  cells were transfected with each plasmid (2.5  $\mu$ g) using 2250 V, 20 ms, 1 pulse. Transfection efficiency was 20–30% for cell lines and 8–12% for primary CLL as assessed by GFP expression.

## Transwell migration and adhesion assays

The experiments were performed as previously described [32, 37]. Migration assays used Corning transwell plates containing  $5 \times 10^5$  cells and 8  $\mu$ m insert (cell lines) and  $1 \times 10^6$  cells and 5  $\mu$ m insert (CLL), and SDF1 $\alpha$  (3 h). Adhesion assays used  $5 \times 10^4$  HS-5 cells/well and  $5 \times 10^6$  primary CLL cells/well (24 h). Migrated/non-migrated fractions and adhered/non-adhered fractions were collected and counted by flow cytometry gating on live B cells.

## Microscopy-based chemokinesis and chemotaxis assays

For chemokinesis assays,  $\mu$ -Slide 8-well chamber slides (Ibidi) were coated with 1  $\mu$ g/ml VCAM-1 at 4  $^{\circ}$ C overnight and washed with warm RPMI1640.  $1 \times 10^5$  Ramos cells were added to allow adhesion (0.5 h), then incubated with the inhibitors (0.5 h) in serum-free medium. After adding SDF1 $\alpha$ , migration was assessed by time-lapse imaging. For chemotaxis assays,  $\mu$ -Slide Chemotaxis<sup>3D</sup> chambers were pre-warmed to 37  $^{\circ}$ C prior to addition of cell/collagen mixtures. Collagen gel mixtures (1.7 mg/ml) were made using PureCol Bovine Collagen (Advanced Biomatrix) and kept on ice [38]. JVM3 cells ( $3 \times 10^6$ /ml) and inhibitors were added, and the mixture was loaded into the chambers. Cell migration was recorded by Zeiss AxioObserver confocal microscope equipped with environmental control (37  $^{\circ}$ C, 5% CO<sub>2</sub>).

## Cell tracking and data analysis

Movement of individual cells, tracked using IMARIS 8.0 software, was quantitatively evaluated by (1) Chemotactic Index [ratio of the displacement of cells toward the chemokine gradient ( $\Delta y$ ) to the total migration distance ( $d$ ) using the equation  $C.I. = \Delta y/d$ , presented as the average value  $\pm$  standard error of the mean (SEM)]; (2) average cell migration speed ( $d/\Delta t$ ; average value  $\pm$  SEM of all cells). (3) Magnitude of velocity (track displacement/ $\Delta t$ ). (4) Mean

square displacement plots cell displacement as a function of time as a measure of migration persistence.

## Intracellular staining, morphological scoring, and confocal microscopy

Ramos cells were added to VCAM-1-coated chamber slides to allow adhesion (0.5 h) then incubated with the inhibitors (0.5 h) in serum-free medium. Cells were then stimulated (SDF1 $\alpha$ ) for the indicated time, fixed (2% PFA), permeabilized (0.5% saponin), washed and stained for F-actin using Alexa Fluor<sup>®</sup> 488 phalloidin (33 nM). Images were taken by Zeiss AxioObserver confocal microscope under 63 $\times$  magnification.

## Statistical analysis

Unless indicated otherwise, Student's *t*-test was used to calculate statistical significance ( $*p < 0.05$ ,  $**p < 0.01$ ,  $***p < 0.001$ ). Error bars represent SEM.

## Results

### Inhibition of PI3K $\gamma$ impairs cell migration to a similar extent as PI3K $\delta$ inhibition

Inhibition of PI3K $\delta$  impairs malignant B cell adhesion and migration [32, 39]; however, the role of PI3K $\gamma$  in this context is unknown. To assess the roles of each PI3K isoform in the regulation of CLL cell migration, we have used isoform-specific inhibitors CZC24832 (PI3K $\gamma$ -specific), GS-1101/idelalisib (PI3K $\delta$ -specific), and dual PI3K $\delta$ /PI3K $\gamma$  inhibitor IPI-145/duvelisib. Pan-PI3K inhibitor GDC-0980/apitolisib was used as a positive control. JVM3 cells, maintained in medium or stimulated for 24 h with CD40L/IL-4, were pre-incubated (1 h) with CZC24832, idelalisib, duvelisib, or GDC-0980. Migration capacity was assessed using a transwell chamber containing SDF1 $\alpha$  in the bottom chamber and the inhibitors in both top and bottom chambers to ensure continued inhibition during the assay. We found that PI3K $\gamma$  inhibition significantly reduced the migration of stimulated JVM3 cells to a similar extent as PI3K $\delta$  inhibition (Fig. 1a). Dual PI3K $\delta$ /PI3K $\gamma$  inhibition further decreased JVM3 cell migration to a level comparable to pan-PI3K inhibition (Fig. 1A). Western blot analysis revealed that CZC24832 reduced SDF1 $\alpha$ -induced phosphorylation of Akt in a dose-dependent manner (Fig. 1B).

We then assessed the sensitivity of CLL cell migration to these inhibitors under the same conditions and observed that PI3K $\gamma$  inhibition alone is sufficient to significantly decrease CLL cell migration, with or without CD40L/IL-4 pre-stimulation (Fig. 2A–C). PI3K $\gamma$  or PI3K $\delta$  inhibitors reduced CLL migration to a similar extent, whereas dual

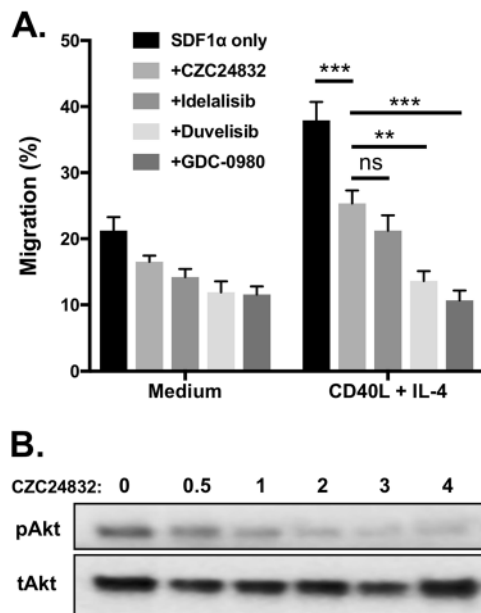
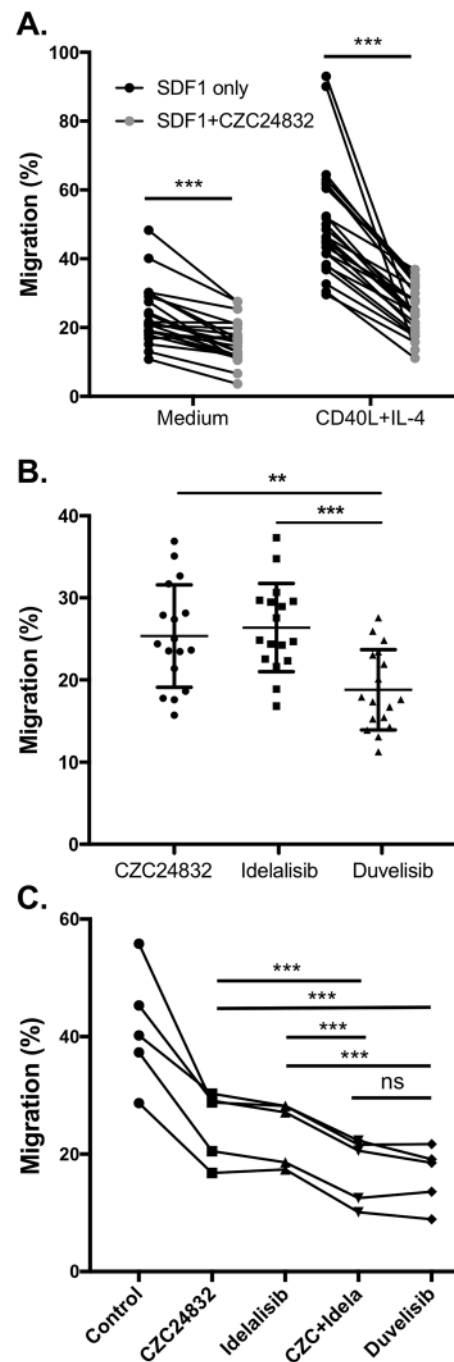


**Fig. 1** Inhibition of PI3K $\gamma$  impairs Akt phosphorylation and B cell migration in a transwell assay. **a** Inhibition of PI3K $\gamma$  or PI3K $\delta$  significantly decreased the migration of JVM3 cells. JVM3 cells were cultured in medium or stimulated for 24 h with CD40L/IL-4 and then incubated with the PI3K $\gamma$ -specific inhibitor CZC24832 (2  $\mu$ M), the PI3K $\delta$ -specific inhibitor idelalisib (1  $\mu$ M), dual PI3K $\delta/\gamma$  inhibitor duvelisib (1  $\mu$ M), or the pan-PI3K inhibitor GDC0980 (1  $\mu$ M) and subjected to a transwell migration assay. DMSO served as the vehicle control for the inhibitors, while SDF1 $\alpha$  (100 ng/ml) served as the chemoattractant ( $n = 7$ ). **b** Effect of PI3K $\gamma$  inhibitor on Akt phosphorylation. JVM3 cells were pre-incubated with the indicated concentrations of CZC4832 (in  $\mu$ M) and then stimulated with SDF1 $\alpha$  for 10 min. Akt Ser473 phosphorylation and total Akt levels were assessed by Western blot

inhibition with duvelisib had a significantly greater impact on migration than PI3K $\gamma$  inhibition alone (Fig. 2A–B). Moreover, the combination of CZC24832 and idelalisib had a significantly greater effect on CLL migration than either inhibitor alone (Fig. 2C). Grouping CLL patients based on major prognostic markers showed that PI3K $\gamma$  inhibition sensitivity was similar in progressive and indolent disease groups defined by ZAP70 or IgVH mutation status (Fig. S2). Consistent with these functional data, PI3K $\gamma$  inhibition reduced phosphorylation of Akt and its downstream targets GSK3 $\beta$  and S6 kinase in CLL cells and greater inhibition was observed with dual PI3K $\delta$ /PI3K $\gamma$  inhibition (Fig. S3A). Inhibitor treatments did not affect relative expression of different PI3K isoforms (Fig. S3B) or cell viability (Fig. S4). Migration of normal human B cells was also significantly impaired by idelalisib, duvelisib, and GDC-0980, whereas PI3K $\gamma$  inhibitor had a relatively small effect that did not reach statistical significance (Fig. S5). Together, these results provide the first demonstration that PI3K $\gamma$  has a non-redundant role in CLL cell migration, and suggest that combined PI3K $\gamma$  and PI3K $\delta$  targeting may in some contexts have a greater impact than targeting either isoform alone.



### Knockdown of p110 $\gamma$ significantly reduced CLL cell migration

We employed CRISPRi technology to provide an independent means of assessing the importance of PI3K $\gamma$  in CLL cell migration. Two guide RNAs were designed targeting different sites of the p110 $\gamma$  gene, and co-expressed with dCas9-GFP in malignant B cell lines Ramos and JVM3. This method was sufficient to significantly and specifically reduce p110 $\gamma$  expression as determined by qPCR analysis of p110 subunit expression (Fig. 3A and



**Fig. 2** Inhibition of PI3K $\gamma$  or PI3K $\delta$  impairs CLL cell migration. **a** Effect of PI3K $\gamma$  inhibitor on CLL cell migration. CLL cells were cultured in medium or stimulated with CD40L+IL-4 for 24 h and subjected to a transwell migration assay. Graphs represent migration of cells from individual CLL patient samples with or without addition of PI3K $\gamma$  inhibitor CZC24832, connected by lines. **b** Inhibition of PI3K $\gamma$  or PI3K $\delta$  decreases the migration of CLL cells to a similar extent, while dual PI3K $\delta/\gamma$  inhibition using duvelisib has significantly greater effect than PI3K $\gamma$  inhibitor alone. **c** Combination of PI3K $\gamma$  inhibitor and PI3K $\delta$  inhibitor decreases the migration of CLL cells to a greater extent than either inhibitor alone. Lines connect individual patient sample migration responses in the presence of the indicated inhibitors. Note all inhibitor-treated groups were significantly different than the control untreated group, whereas the CZC24832+idelalisib combination was not significantly different than duvelisib.

Fig. S6A). Following a 48 h recovery period, transfected cells were assessed for migration using a transwell assay. We observed that p110 $\gamma$  downregulation significantly reduced cell migration compared to control cells (Fig. 3B). Moreover, knockdown of p110 $\gamma$  in primary CLL cells significantly reduced their migration independently of IgVH mutation status (Fig. 3C) and ZAP70 expression (Fig. S6B), without compromising cell viability (Fig. S4B). These results are consistent with those seen with PI3K $\gamma$  inhibition, and confirm that PI3K $\gamma$  has an independent and essential function in malignant B cell migration.

### Expression of PI3K $\gamma$ in CLL cells is enhanced in response to CD40L/IL-4 stimulation independently of ZAP70 status or IgVH mutation

We examined the expression of PI3K $\gamma$  subunits in CLL prognostic groups and determined whether PI3K $\gamma$  expression is influenced by BCR cross-linking or stimulation with T cell-derived factors. Purified CLL cells were stimulated (24 h) with  $\alpha$ -IgM or CD40L/IL-4 and mRNA abundance of p110 $\gamma$  and p101 were determined. We observed that the expression of p110 $\gamma$  mRNA was significantly upregulated after CD40L/IL-4 stimulation, but not after  $\alpha$ -IgM stimulation, regardless of ZAP70 or IgVH mutation status (Fig. 4A and Fig. S7A). Both  $\alpha$ -IgM and CD40L/IL-4 stimulation were able to activate the PI3K kinase signaling pathway in CLL (Fig. S8). Expression of p101 was highly heterogeneous, but the majority of CLL patients showed increased p101 expression after CD40L/IL-4 stimulation (Fig. 4B and Fig. S7B). Interestingly, a few patients who expressed p101 at high levels without stimulation showed the reverse trend (Fig. S7B), suggesting that distinct mechanisms may maintain high p101 expression in these patients. Examination of p110 $\gamma$  and p101 protein expression also indicated heterogeneity and a trend of increased expression after CD40L/IL-4 stimulation (Fig. 4C). Analysis of microarray data generated from leukemic B cells isolated from CLL patient peripheral blood or lymph nodes

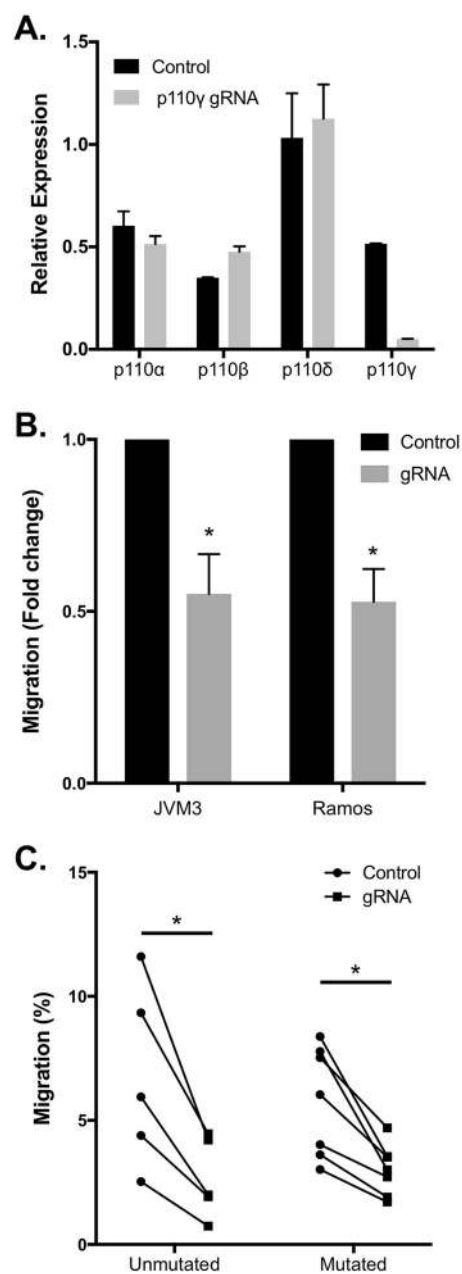


**Fig. 3** The effect of CRISPRi knockdown of p110 $\gamma$  on the migration of malignant B cell lines and CLL cells. **a** Confirmation of p110 $\gamma$  CRISPRi knockdown specificity. JVM3 cells were transfected with either dCas9-GFP expression vector alone (Control) or co-transfected with dCas9-GFP plus vectors expressing p110 $\gamma$ -targeting guide RNAs (at a 1:3 ratio). After 24 h, p110 isoform expression within sorted GFP+ transfectants was assessed by qPCR. **b** p110 $\gamma$  knockdown significantly impaired the migration of JVM3 and Ramos cells. Cells were transfected as above and then subjected to a transwell migration assay. Data represent average fold change in migration of GFP+ cells ( $n = 3$ ). **c** p110 $\gamma$  knockdown significantly reduced the migration of primary CLL cells regardless of their IgVH mutation status. CLL cells were transfected with either dCas9-GFP expression vector or dCas9-GFP plus vectors expressing p110 $\gamma$ -targeting guide RNAs then assessed 48 h later using a transwell migration assay. Percent of cells migrating toward SDF1 $\alpha$  was determined by flow cytometry counting of live GFP-expressing cells present in the upper and lower chambers after 3 h

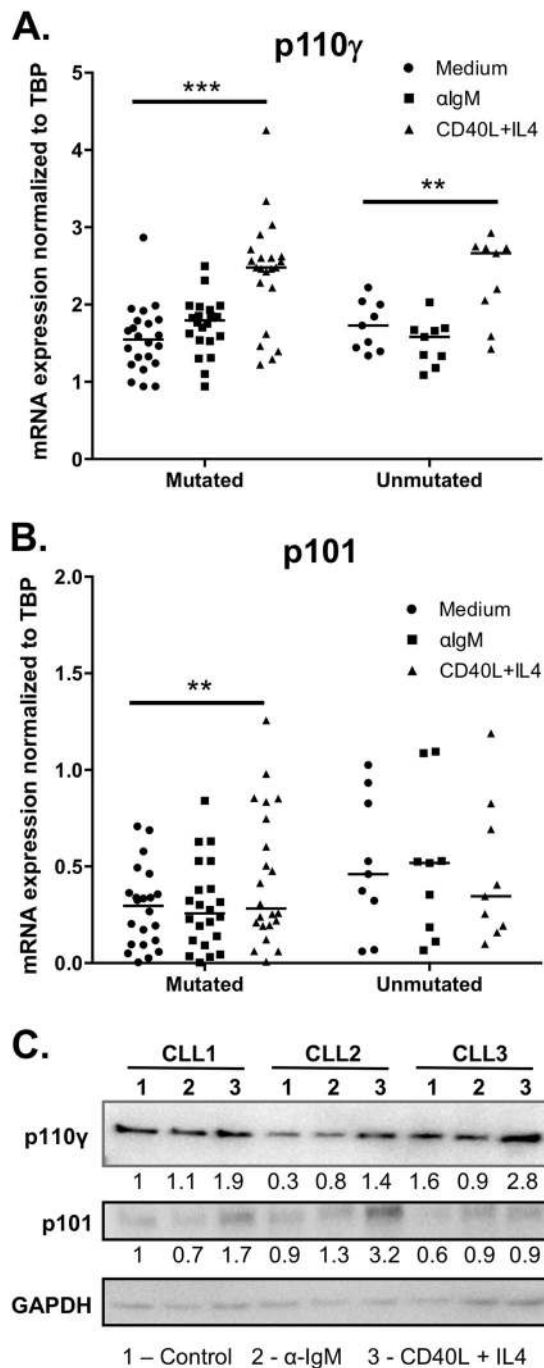


**Fig. 4** Expression of PI3K $\gamma$  subunits in malignant B cell lines and CLL patient samples. **a**, **b** CLL cells were stimulated with F(ab')<sub>2</sub>  $\alpha$ -IgM (10  $\mu$ g/ml) or CD40L/IL-4 (50 ng/ml each) and harvested 24 h later for RNA extraction and RT-qPCR analysis. mRNA expression of **a** p110 $\gamma$  and **b** p101 were determined, and expression levels were normalized against the expression of TATA box-binding protein (TBP). Patients were divided into indolent vs. progressive groups based on IgVH mutation status. **c** Protein expression of p110 $\gamma$  and p101 in CLL samples in response to BCR stimulation or CD40L/IL-4 stimulation. Data are representative of nine patients analyzed

(GEO data set GDS4176; [40]) revealed that both p110 $\gamma$  and p101 are more highly expressed in lymph node than

peripheral blood (Fig. S9). Together, these results indicate that CLL cells express PI3K $\gamma$  and its expression can be modulated by factors present in the lymphoid tissue microenvironment.

### Overexpression of PI3K $\gamma$ enhances chemokine-induced cell migration

To determine whether increased PI3K $\gamma$  expression can impact the migration of CLL cells, p110 $\gamma$  or p101 subunits were each overexpressed in JVM3 cells. After transfection with either p110 $\gamma$ -GFP or p101-GFP expression plasmids, overexpression was confirmed by qPCR (Fig. 5A). Migration of the transfected cells was measured using the trans-well assay. We found that chemokine-induced migration of JVM3 cells is significantly increased by overexpression of either p110 $\gamma$  or p101 (Fig. 5B). We further determined the impact of PI3K $\gamma$  subunits on migration of CLL cells. While overexpression of p101 did not increase CLL migration, overexpression of p110 $\gamma$  resulted in significant but variable increases in migration (Fig. 5C). Co-expression of both p110 $\gamma$  and p101 significantly increased migration in the majority of CLL patient samples, and had a significantly greater impact than expression of p110 $\gamma$  alone (Fig. 5C). Together these data support the importance of PI3K $\gamma$  in CLL cell migration and suggest that its expression level is an important factor determining cellular migration capacity.

### Impact of PI3K $\gamma$ or PI3K $\delta$ inhibition on cell migration behavior within chemokine gradients

Unlike PI3K $\delta$ , PI3K $\gamma$  is known to directly associate with G-protein-coupled receptors via binding to activated G $\beta$ / $\gamma$  subunits [25, 41] and can mediate directional migration within chemokine gradients [29, 30, 42]. To determine whether PI3K $\gamma$  and PI3K $\delta$  may affect distinct migration behaviors, cells were observed by video microscopy and migration analyzed by cell tracking software. We first measured migration of Ramos cells plated on a VCAM-1-coated glass surface and stimulated with SDF1 $\alpha$  and found that inhibition of either PI3K $\gamma$  or PI3K $\delta$  impair migration velocity (Fig. S10A) and mean squared displacement [33], a measure of directional migration persistence (Fig. S10B). We then assessed migration within a microfluidic device containing an SDF1 $\alpha$  gradient within a collagen gel to allow determination of the chemotactic index, a measure of directional migration reflecting the ability of cells to detect the chemokine gradient [43]. Analyses of JVM3 cell migration tracks within this gradient system (Fig. 6A) revealed that either PI3K $\delta$  or PI3K $\gamma$  inhibition were sufficient to reduce the chemotactic index (Fig. 6B) and migration velocity (Fig. 6C) under these conditions, with PI3K $\gamma$  inhibition showing the strongest effect.

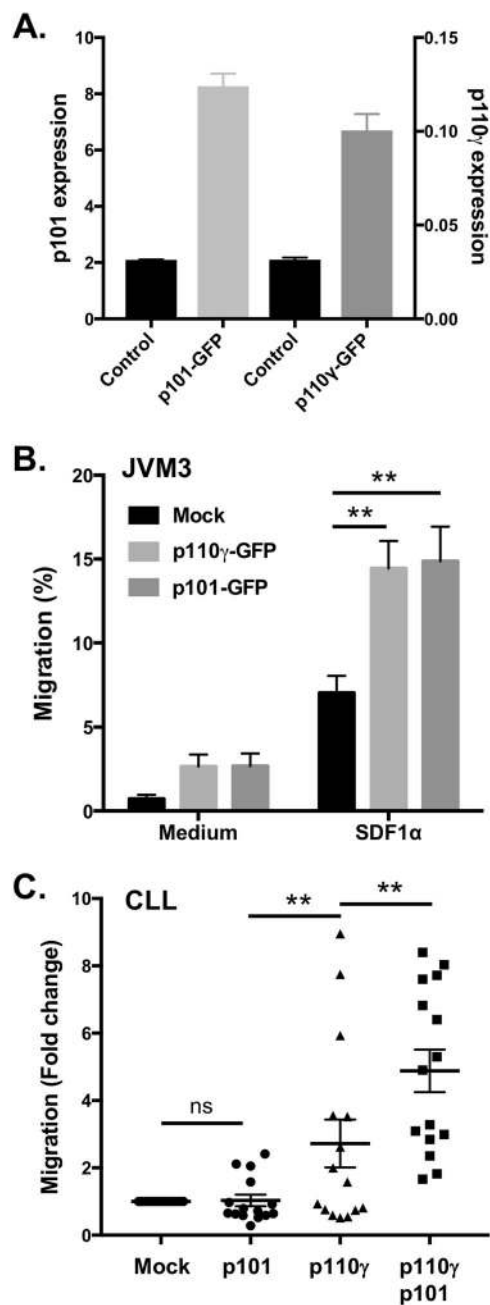


**Fig. 5** Overexpression of PI3K $\gamma$  subunits affects the migration of malignant B cells. **a** Confirmation of p110 $\gamma$ -GFP and p101-GFP overexpression in JVM3 cells. JVM3 cells were transfected with either p101-GFP or p110 $\gamma$ -GFP plasmids. 24 h post transfection, RNA was harvested and expression of p101 or p110 $\gamma$  was determined by RT-qPCR analysis. **b** Overexpression of p110 $\gamma$  or p101 enhances the migration of JVM3 in response to the chemokine SDF1 $\alpha$ . 24 h after transfection with p101-GFP plasmid or p110 $\gamma$ -GFP, migration of live GFP-expressing cells in response to SDF1 $\alpha$  (100 ng/ml) was assessed using a transwell migration assay. The graph shows the mean and SEM of four experiments. **c** Overexpression of PI3K $\gamma$  subunits enhances CLL cell migration. p110 $\gamma$ -GFP, p101-GFP, or both together were overexpressed in CLL cells. After 48 h, migration of live GFP+ cells was assessed by transwell assays as above. Results are expressed as fold change in migration relative to the control transfection of the same patient sample

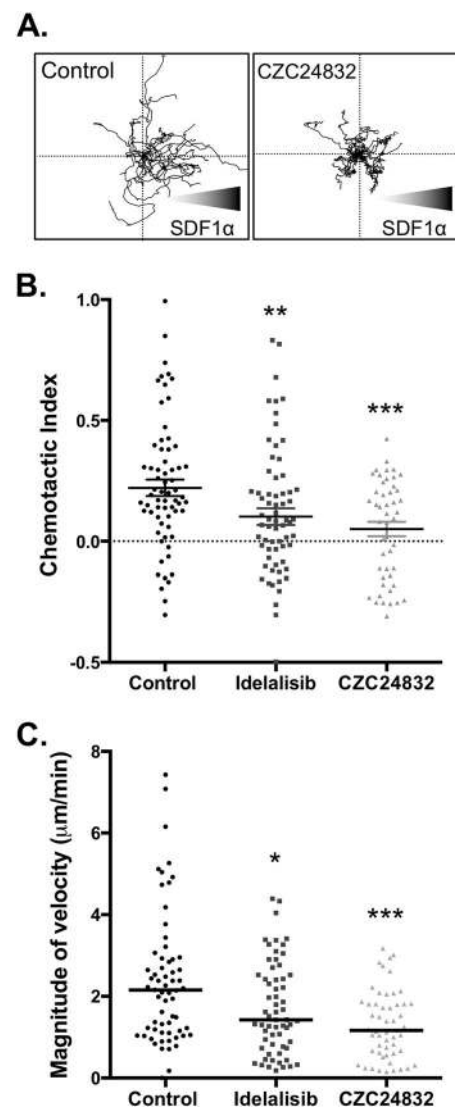


**Fig. 6** Impact of PI3K $\gamma$  or PI3K $\delta$  inhibition on directional migration behavior. JVM3 cells were seeded into a collagen gel and treated with the indicated inhibitors for 60 min. After establishing the SDF1 $\alpha$  gradient, time-lapse imaging was performed and cell migration tracks were analyzed using the IMARIS 8.0 software. **a** Plots illustrate cell tracks from a single representative experiment, overlaid to the same origin. Note that cells treated with CZC24843 show visibly impaired chemotaxis toward the higher SDF1 $\alpha$  concentration (right half of the graphs). **b–c** Quantitative analysis of cell tracks showing that both PI3K $\delta$  and PI3K $\gamma$  inhibition reduced the chemotactic index **b** and migration velocity **c**. Mann–Whitney test, \*\* $p < 0.01$ ; \*\*\* $p < 0.001$

### PI3K $\gamma$ or PI3K $\delta$ inhibition differentially affect cytoskeletal remodeling and cell morphology

We noted that PI3K $\gamma$  inhibitor-treated cells frequently show abnormal morphologies after SDF1 $\alpha$  stimulation, including dynamic multiple protrusions that fail to develop into fully polarized leading edges (Fig. 7A). We microscopically scored cells exhibiting round, elongated, polarized, or multi-protrusion morphologies by fixing cells after 1 min of SDF1 $\alpha$

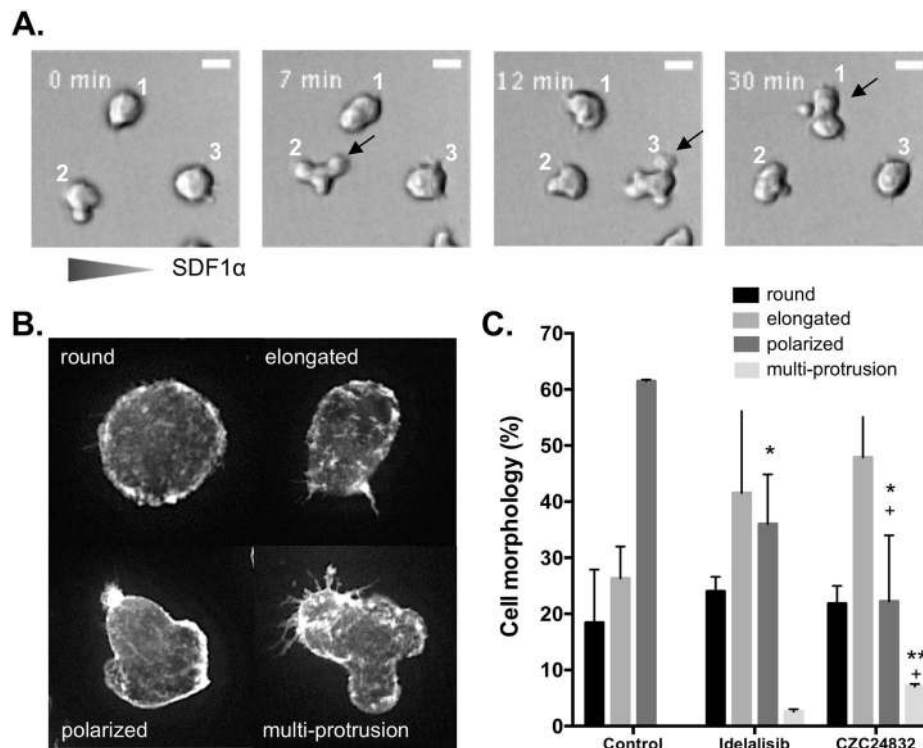


**Fig. 7** PI3K $\delta$  and PI3K $\gamma$  inhibitors differentially affect cytoskeletal remodeling and cell morphology. **a** Time-lapse images of CZC24832-treated Ramos cells migrating within SDF1 $\alpha$  gradient, showing the dynamic formation and retraction of multiple protrusions and failure to form a stable polarized morphology. Note that all three cells in this field exhibit multiple protrusions at one of the time points (indicated by arrows) and failed to migrate significantly in the direction of the SDF1 $\alpha$  gradient. **b** Morphological scoring demonstrating the differential impact of PI3K $\delta$  and PI3K $\gamma$  inhibitors on Ramos cell

polarization. Ramos cells were pretreated with inhibitors, stimulated with 100 ng/ml SDF1 $\alpha$  for 1 min, then fixed and F-actin stained using Alexa-488 phalloidin. Representative CZC24832-treated cells exhibiting the four major observed morphologies are shown. **c** Frequency of cells exhibiting each morphology within control and inhibitor-treated groups. Data are based on three independent experiments scoring over 200 cells per treatment group in total. Paired *t*-test, asterisk denotes significance comparing drug-treated to control, plus denotes significance comparing CZC24832 to Idelalisib

stimulation and staining the F-actin cytoskeleton (Fig. 7B). It was found that either PI3K $\delta$  or PI3K $\gamma$  inhibition was sufficient to reduce the proportion of fully polarized cells and increase the proportion of elongated or multi-protrusion morphologies; however, PI3K $\gamma$  inhibition decreased polarization and increased multi-protrusion morphologies to a greater extent than PI3K $\delta$  inhibition (Fig. 7C). Together these results indicate a unique and non-redundant role for PI3K $\gamma$  in mediating chemokine-induced alterations in the cytoskeleton and chemokine gradient sensing.

**Inhibition of either PI3K $\gamma$  or PI3K $\delta$  significantly decreases the adhesion of CLL cells to bone marrow-derived stromal cells**

Adhesion of CLL cells to stromal cells is driven by chemokines such as SDF1 $\alpha$  and promotes their retention and interaction with other cell types present in the lymphoid tissue microenvironment [2, 32]. To determine the roles of PI3K $\gamma$  and PI3K $\delta$  in the interaction of CLL cells and stromal cells, we co-cultured CLL cells with human stromal

cell line HS-5 with or without specific PI3K inhibitors. After 24 h, the non-adhered CLL cells were collected and then adhered cells along with the stromal cells were removed using trypsin. CD19-expressing cells in the adhered and non-adhered fractions were counted by flow cytometry and the adhesion index was calculated accordingly. We found that PI3K $\gamma$  inhibition significantly reduced binding to stromal cells, and dual inhibition of PI3K $\gamma$  and PI3K $\delta$  had a stronger effect than PI3K $\gamma$  inhibition alone (Fig. 8A). While basal adhesion to stromal cells was higher in ZAP70 + CLL cells as expected, the inhibition of either PI3K $\gamma$  or PI3K $\delta$  significantly decreased CLL cell adhesion in both ZAP70+ and ZAP70- groups (Fig. 8B). In both patient groups, duvelisib had a stronger effect than either single isoform inhibitor (Fig. 8B–C). These differences in response to the inhibitors were not due to differences in cell viability as we did not see noticeable effect of the inhibitors on CLL cell survival under these conditions (Fig. S4). These results indicate that PI3K $\gamma$  also contributes to chemokine-dependent and integrin-dependent adhesion of CLL cells to stromal cells.



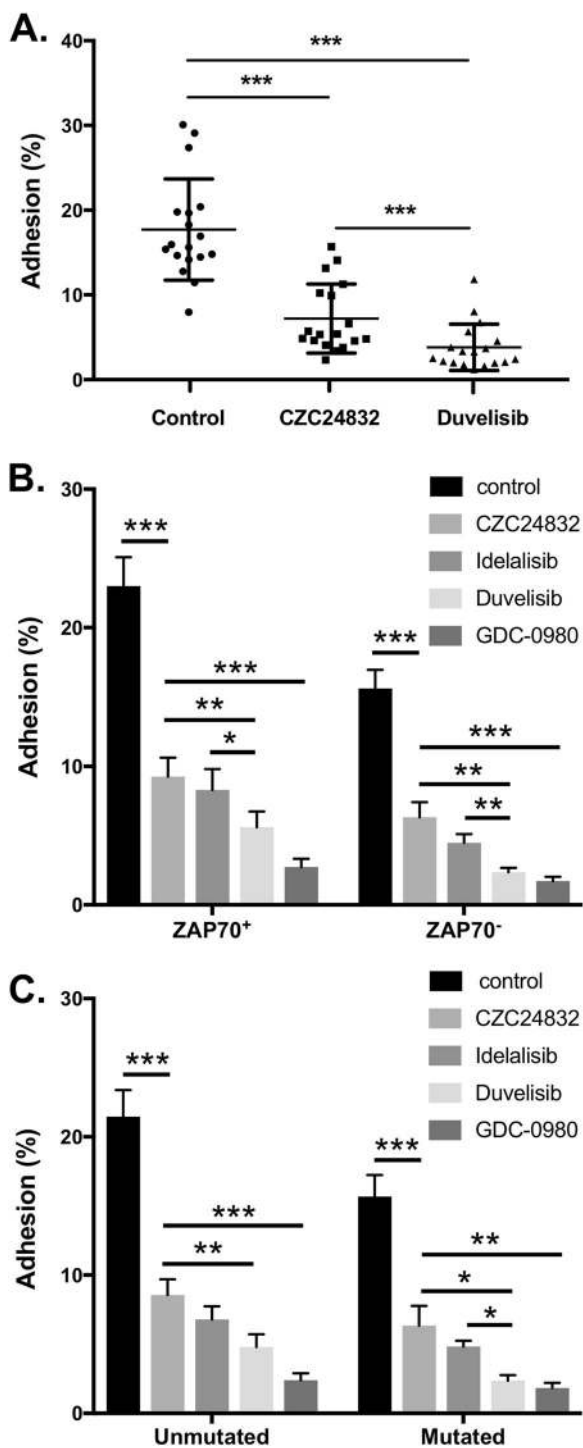


**Fig. 8** Inhibition of either PI3K $\gamma$  or PI3K $\delta$  significantly decreases the adhesion of CLL cells to stromal cells without affecting CLL cell survival. CLL cells were incubated for 24 h with established monolayers of human stromal cell line HS-5 in the presence of the indicated inhibitors. The adhered and non-adhered CLL cell fractions were counted by flow cytometry, gating on the live cell population expressing CD19, to determine the percent adhesion. **a** Impact of PI3K $\gamma$  or PI3K $\gamma$ /PI3K $\delta$  dual inhibitors on stromal cell binding. The graph displays percent adhesion of individual CLL patient samples under different inhibitor treatment conditions. Inhibition of PI3K $\gamma$  or PI3K $\delta$  significantly decreased the adhesion of CLL cells regardless of **b** ZAP70 status or **c** IgVH mutation status

the PI3K $\delta$ -specific inhibitor idelalisib that has shown significant activity in this disease [44]. Idelalisib deprives CLL cells of essential survival and proliferative stimuli received from the resident cells of the microenvironment, thus reducing lymphadenopathy and causing egress of CLL cells into peripheral blood. Upon egress, CLL cells may be more vulnerable to the conventional therapeutics used in CLL treatment. We and others have shown that idelalisib can significantly reduce malignant B cell migration in response to chemotactic stimuli [39, 45]. Idelalisib was found to affect CLL cell adhesion [32, 46] and may also affect tissue-resident cells capacity for cell–cell interaction and secretion of soluble factors [39].

Unlike protein kinases, all four class I PI3Ks phosphorylate the same target molecules and generate identical D3 phosphoinositide products, thus they are expected to exhibit some functional redundancy. Some level of redundancy may be important to ensure robust activation and fine-tuning of this pathway. One way in which PI3Ks may exhibit unique functions is via differential expression among cell types. PI3K $\delta$  and PI3K $\gamma$  subunits are expressed most abundantly in hematologic cells. It was estimated that PI3K $\delta$  contributes approximately 50% of the total PI3K activity in lymphocytes [47], thus targeting PI3K $\delta$  has a significant impact on lymphocyte functions that are highly dependent on D3 phosphoinositides [48]. In contrast, the contributions of PI3K $\gamma$  have only been clearly defined in T cells and myeloid cells [29, 30, 49]. PI3K $\gamma$ -deficient mice have defective antibody responses upon immunization [30], but this may reflect impaired T cell and myeloid cell function. Moreover, PI3K $\gamma$ -deficient mouse B cells exhibited normal migration to chemokines in transwell assays and did not show altered homing to tissues when transferred to normal hosts [29], leading to the conclusion that PI3K $\gamma$  has a minimal role in B cell migration in mice.

To delineate the respective influence of PI3K $\delta$  and PI3K $\gamma$  in the context of human B cell malignancy, we compared idelalisib to a highly selective PI3K $\gamma$  inhibitor CZC24832 [33]. Both inhibitors were able to significantly reduce CLL migration and adhesion. As these compounds may have differing specificity, potency, and stability, we used several

## Discussion

The PI 3-kinases  $\alpha$ ,  $\beta$ ,  $\gamma$ , and  $\delta$  collectively regulate major signaling pathways promoting CLL cell chemotaxis, cytoskeletal rearrangement, and CLL cell interaction with the microenvironment. A recent addition to CLL therapy is

approaches to confirm selective effects under the conditions of our experiments. A pan-PI3K inhibitor GDC-0980 was found to have stronger effects on both migration and phosphorylation of Akt and its downstream targets than either PI3K $\gamma$ , PI3K $\delta$ , or dual PI3K $\delta/\gamma$  inhibitors. This is consistent with a contribution from PI3K $\alpha/\beta$  isoforms which is not effectively blocked by PI3K $\delta/\gamma$  inhibitors under the conditions of our experiments. We have also observed that pan-PI3K inhibitor but not PI3K $\gamma$  inhibitor can block Akt phosphorylation in stromal cells that do not express PI3K $\gamma$ , further confirming specificity (data not shown). Importantly, we also confirm the key conclusion of the paper regarding PI3K $\gamma$  and CLL migration using the completely independent approach of genetic silencing by CRISPRi.

PI3K $\gamma$  inhibition had a particularly strong effect on directional migration within collagen gels containing an SDF1 $\alpha$  gradient. This suggests an important role of PI3K $\gamma$  in chemokine sensing and cell polarization toward the chemokine gradient, consistent with findings in neutrophils [23, 50, 51]. We also found that PI3K $\gamma$  inhibition had a stronger impact on cell morphology than PI3K $\delta$  inhibition, and led to a reduction in polarization and an increase in abnormal multipolar morphologies upon exposure to a chemokine. We hypothesize that the direct linkage between PI3K $\gamma$  and chemokine receptors, via direct p101–G $\beta\gamma$  interactions, provides a unique and indispensable contribution to efficient chemotaxis, perhaps by controlling spatial gradients of phosphoinositides within the plasma membrane. Together, these results provide the first demonstration that PI3K $\gamma$  has unique non-redundant functions in chemokine-mediated responses in human B cell malignancies.

PI3K $\gamma$  has two unique adapter subunits p84 and p101, distinct from the p85 adapter used by PI3K $\delta$  [52]. Whereas p84 specifically couples PI3K $\gamma$  to signaling pathways controlling oxidative burst in neutrophils [23, 50], p101 can directly couple PI3K $\gamma$  to G $\beta\gamma$  subunits generated by ligand-activated chemokine receptors [53, 54]. We found that CLL cells express p101 but not p84 (data not shown). Both p101 and p110 $\gamma$  catalytic subunits showed increased expression upon activation by CD40L/IL-4 in most CLL patient samples. Consistent with these *in vitro* data, examination of p101 and p110 $\gamma$  expression in a well-annotated microarray data set [40] showed that CLL cells isolated from lymph node express higher levels of PI3K $\gamma$  subunits than CLL cells isolated from blood of the same patients. Moreover, overexpression of p101 and p110 $\gamma$  together significantly enhanced CLL cell migration, suggesting that CLL cell expression of functional PI3K $\gamma$  can be modulated by microenvironmental signals and can functionally impact chemokine receptor-mediated responses.

Studies in mouse and human have revealed multiple roles of PI3K $\gamma$  in immune functions. Animals genetically

deficient in PI3K $\gamma$  do not show obvious defects in B cell functions; however, these mice may have developed compensatory mechanisms such as increased expression of other PI3K isoforms that obscure changes in B cell functions. Moreover, B1 and marginal zone B cells, considered as possible normal counterparts of CLL cells, were not examined in PI3K $\gamma$ -deficient mice. It remains possible that human B cells are more dependent on PI3K $\gamma$  than mouse B cells, or that our findings here may reflect unique properties of B cell malignancies. It is established that PI3K $\gamma$  plays essential roles in normal T, NK, and myeloid cell functions in mice [55]. As a result, PI3K $\gamma$  inhibition or dual PI3K $\delta$  and PI3K $\gamma$  inhibition had anti-inflammatory activities in several disease models in mice, attributed to inhibition of cell migration into inflamed tissues [55, 56]. Since one of the major hurdles in clinical use of idelalisib is T cell-mediated toxicities [57, 58], it is tempting to speculate that dual inhibition of PI3K $\delta$  and PI3K $\gamma$  may partly mitigate these toxicities by impairing T cell migration into sites of inflammation such as colon, lung, or liver.

Dual inhibition of PI3K $\delta$  and PI3K $\gamma$  has been proposed to have potential benefit for CLL treatment and is currently in clinical trials [39, 59, 60]. However, a direct comparison of the relative effectiveness of dual vs. single inhibition has not been reported. We find that dual inhibition has a stronger effect on PI3K/Akt pathway activity, chemokine-dependent migration and adhesion than either PI3K $\delta$  or PI3K $\gamma$  inhibitors. While our findings do not exclude the contribution of other PI3K isoforms, they do provide the first demonstration of a distinct biological function of PI3K $\gamma$  in B cells. Additional blockade of PI3K $\gamma$  may thus improve clinical benefits via increased anti-leukemic activity and reduced T cell-mediated toxicities.

**Acknowledgements** Funding for this work was provided by a grant from the Leukemia and Lymphoma Society of Canada to AJM, SBG, and FL. AJM was supported by a Canada Research Chair. AYA was supported by a fellowship from CancerCare Manitoba and Research Manitoba. XW was supported by a studentship from Research Manitoba and NE by the Children's Hospital Research Institute of Manitoba. JEG was supported by Natural Sciences and Engineering Research Council of Canada and the Canada Foundation for Innovation. TTM was supported by the GSK-CIHR Partnered program and Research Manitoba. The CLL research cluster and tumor bank were supported by Research Manitoba and CancerCare Manitoba. The authors would like to thank Christine Zhang for technical support, Donna Hewitt, Michelle Queau, Mandy Squires, Yun Li, Laurie Lange, and all the Manitoba Blood and Marrow bank staff for management of patient samples and clinical information, and the patients for their blood donations.

**Author contributions** AYA and XW performed research, analyzed data, performed statistical analyses, and wrote the manuscript. NE, SH, and JEG performed research. VB and JBJ designed research and collected vital biomarker and clinical data. FL and TTM contributed vital analytical tools. SBG designed research and analyzed and

interpreted data. AJM designed research, analyzed and interpreted data, supervised trainees, and wrote the manuscript.

## Compliance with ethical standards

**Conflict of interest** The authors declare that they have no conflict of interest.

**Open Access** This article is licensed under a Creative Commons Attribution-NonCommercial-ShareAlike 4.0 International License, which permits any non-commercial use, sharing, adaptation, distribution and reproduction in any medium or format, as long as you give appropriate credit to the original author(s) and the source, provide a link to the Creative Commons license, and indicate if changes were made. If you remix, transform, or build upon this article or a part thereof, you must distribute your contributions under the same license as the original. The images or other third party material in this article are included in the article's Creative Commons license, unless indicated otherwise in a credit line to the material. If material is not included in the article's Creative Commons license and your intended use is not permitted by statutory regulation or exceeds the permitted use, you will need to obtain permission directly from the copyright holder. To view a copy of this license, visit <http://creativecommons.org/licenses/by-nc-sa/4.0/>.

## References

1. Stevenson FK, Krysov S, Davies AJ, Steele AJ, Packham G. B-cell receptor signaling in chronic lymphocytic leukemia. *Blood*. 2011;118:4313–20.
2. Burger JA, Gribben JG. The microenvironment in chronic lymphocytic leukemia (CLL) and other B cell malignancies: insight into disease biology and new targeted therapies. *Semin Cancer Biol*. 2014;24:71–81.
3. Lagneaux L, Delforge A, Bron D, De Bruyn C, Stryckmans P. Chronic lymphocytic leukemic B cells but not normal B cells are rescued from apoptosis by contact with normal bone marrow stromal cells. *Blood*. 1998;91:2387–96.
4. Munk Pedersen I, Reed J. Microenvironmental interactions and survival of CLL B-cells. *Leuk Lymphoma*. 2004;45:2365–72.
5. Burger JA, Ghia P, Rosenwald A, Caligaris-Cappio F. The microenvironment in mature B-cell malignancies: a target for new treatment strategies. *Blood*. 2009;114:3367–75.
6. Crespo M, Bosch F, Villamor N, Bellosillo B, Colomer D, Rozman M, et al. ZAP-70 expression as a surrogate for immunoglobulin-variable-region mutations in chronic lymphocytic leukemia. *N Engl J Med*. 2003;348:1764–75.
7. Preobrazhensky SN, Szankasi P, Bahler DW. Improved flow cytometric detection of ZAP-70 in chronic lymphocytic leukemia using experimentally optimized isotopic control antibodies. *Cytom B Clin Cytom*. 2012;82:78–84.
8. Durig J, Nuckel H, Cremer M, Fuhrer A, Halfmeyer K, Fandrey J, et al. ZAP-70 expression is a prognostic factor in chronic lymphocytic leukemia. *Leukemia*. 2003;17:2426–34.
9. Stilgenbauer S. Prognostic markers and standard management of chronic lymphocytic leukemia. *Hematology Am Soc Hematol Educ Program*. 2015;2015:368–77.
10. Deaglio S, Vaisitti T, Aydin S, Bergui L, D'Arena G, Bonello L, et al. CD38 and ZAP-70 are functionally linked and mark CLL cells with high migratory potential. *Blood*. 2007;110:4012–21.
11. Lafarge ST, Li H, Pauls SD, Hou S, Johnston JB, Gibson SB, et al. ZAP70 expression directly promotes chronic lymphocytic leukaemia cell adhesion to bone marrow stromal cells. *Br J Haematol*. 2015;168:139–42.
12. Richardson SJ, Matthews C, Catherwood MA, Alexander HD, Carey BS, Farrugia J, et al. ZAP-70 expression is associated with enhanced ability to respond to migratory and survival signals in B-cell chronic lymphocytic leukemia (B-CLL). *Blood*. 2006;107:3584–92.
13. Cheng JQ, Godwin AK, Bellacosa A, Taguchi T, Franke TF, Hamilton TC, et al. AKT2, a putative oncogene encoding a member of a subfamily of protein-serine/threonine kinases, is amplified in human ovarian carcinomas. *Proc Natl Acad Sci USA*. 1992;89:9267–71.
14. Kandel ES, Hay N. The regulation and activities of the multi-functional serine/threonine kinase Akt/PKB. *Exp Cell Res*. 1999;253:210–29.
15. Testa JR, Bellacosa A. AKT plays a central role in tumorigenesis. *Proc Natl Acad Sci USA*. 2001;98:10983–5.
16. Nicholson KM, Anderson NG. The protein kinase B/Akt signaling pathway in human malignancy. *Cell Signal*. 2002;14:381–95.
17. Vivanco I, Sawyers CL. The phosphatidylinositol 3-Kinase AKT pathway in human cancer. *Nat Rev Cancer*. 2002;2:489–501.
18. Brown JR, Byrd JC, Coutre SE, Benson DM, Flinn IW, Wagner-Johnston ND, et al. Idelalisib, an inhibitor of phosphatidylinositol 3-kinase p110delta, for relapsed/refractory chronic lymphocytic leukemia. *Blood*. 2014;123:3390–7.
19. Wei M, Wang X, Song Z, Jiao M, Ding J, Meng LH, et al. Targeting PI3Kdelta: emerging therapy for chronic lymphocytic leukemia and beyond. *Med Res Rev*. 2015;35:720–52.
20. Till KJ, Pettitt AR, Slupsky JR. Expression of functional sphingosine-1 phosphate receptor-1 is reduced by B cell receptor signaling and increased by inhibition of PI3 kinase delta but not SYK or BTK in chronic lymphocytic leukemia cells. *J Immunol*. 2015;194:2439–46.
21. Barrientos JC. Idelalisib for the treatment of chronic lymphocytic leukemia/small lymphocytic lymphoma. *Future Oncol*. 2016;12:2077–94.
22. Bohnacker T, Marone R, Collmann E, Calvez R, Hirsch E, Wymann MP. PI3Kgamma adaptor subunits define coupling to degranulation and cell motility by distinct PtdIns(3,4,5)P3 pools in mast cells. *Sci Signal*. 2009;2:ra27.
23. Deladeriere A, Gambardella L, Pan D, Anderson KE, Hawkins PT, Stephens LR. The regulatory subunits of PI3Kgamma control distinct neutrophil responses. *Sci Signal*. 2015;8:ra8.
24. Brazzatti JA, Klingler-Hoffmann M, Haylock-Jacobs S, Harata-Lee Y, Niu M, Higgins MD, et al. Differential roles for the p101 and p84 regulatory subunits of PI3Kgamma in tumor growth and metastasis. *Oncogene*. 2012;31:2350–61.
25. Vadas O, Dbouk HA, Shymanets A, Perisic O, Burke JE, Abi Saab WF, et al. Molecular determinants of PI3Kgamma-mediated activation downstream of G-protein-coupled receptors (GPCRs). *Proc Natl Acad Sci USA*. 2013;110:18862–7.
26. Turvey ME, Klingler-Hoffmann M, Hoffmann P, McColl SR. p84 forms a negative regulatory complex with p110gamma to control PI3Kgamma signalling during cell migration. *Immunol Cell Biol*. 2015;93:735–43.
27. Thomas MS, Mitchell JS, DeNucci CC, Martin AL, Shimizu Y. The p110gamma isoform of phosphatidylinositol 3-kinase regulates migration of effector CD4 T lymphocytes into peripheral inflammatory sites. *J Leukoc Biol*. 2008;84:814–23.
28. Martin AL, Schwartz MD, Jameson SC, Shimizu Y. Selective regulation of CD8 effector T cell migration by the p110 gamma isoform of phosphatidylinositol 3-kinase. *J Immunol*. 2008;180:2081–8.

29. Reif K, Okkenhaug K, Sasaki T, Penninger JM, Vanhaesebroeck B, Cyster JG. Cutting edge: differential roles for phosphoinositide 3-kinases, p110 $\gamma$  and p110 $\delta$ , in lymphocyte chemotaxis and homing. *J Immunol*. 2004;173:2236–40.
30. Sasaki T, Irie-Sasaki J, Jones RG, Oliveira-dos-Santos AJ, Stanford WL, Bolon B, et al. Function of PI3K $\gamma$  in thymocyte development, T cell activation, and neutrophil migration. *Science*. 2000;287:1040–6.
31. Dong S, Guinn D, Dubovsky JA, Zhong Y, Lehman A, Kutok J, et al. IPI-145 antagonizes intrinsic and extrinsic survival signals in chronic lymphocytic leukemia cells. *Blood*. 2014;124:3583–6.
32. Lafarge ST, Johnston JB, Gibson SB, Marshall AJ. Adhesion of ZAP-70+ chronic lymphocytic leukemia cells to stromal cells is enhanced by cytokines and blocked by inhibitors of the PI3-kinase pathway. *Leuk Res*. 2014;38:109–15.
33. Bergamini G, Bell K, Shimamura S, Werner T, Cansfield A, Muller K, et al. A selective inhibitor reveals PI3K $\gamma$  dependence of T (H)17 cell differentiation. *Nat Chem Biol*. 2012;8:576–82.
34. Ali AY, Abedini MR, Tsang BK. The oncogenic phosphatase PPM1D confers cisplatin resistance in ovarian carcinoma cells by attenuating checkpoint kinase 1 and p53 activation. *Oncogene*. 2012;31:2175–86.
35. Eissa N, Hussein H, Wang H, Rabbi MF, Bernstein CN, Ghia JE. Stability of reference genes for messenger RNA quantification by real-time PCR in mouse dextran sodium sulfate experimental colitis. *PLoS ONE*. 2016;11:e0156289.
36. Gilbert LA, Horlbeck MA, Adamson B, Villalta JE, Chen Y, Whitehead EH, et al. Genome-scale CRISPR-mediated control of gene repression and activation. *Cell*. 2014;159:647–61.
37. Li H, Hou S, Wu X, Nandagopal S, Lin F, Kung S, et al. The tandem PH domain-containing protein 2 (TAPP2) regulates chemokine-induced cytoskeletal reorganization and malignant B cell migration. *PLoS ONE*. 2013;8:e57809.
38. Foley MH, Forcier T, McAndrew E, Gonzalez M, Chen H, Juelg B, et al. High avidity CD8(+) T cells efficiently eliminate motile HIV-infected targets and execute a locally focused program of anti-viral function. *PLoS ONE*. 2014;9:e87873.
39. Hoellenriegel J, Meadows SA, Sivina M, Wierda WG, Kantarjian H, Keating MJ, et al. The phosphoinositide 3'-kinase delta inhibitor, CAL-101, inhibits B-cell receptor signaling and chemokine networks in chronic lymphocytic leukemia. *Blood*. 2011;118:3603–12.
40. Herishanu Y, Perez-Galan P, Liu D, Biancotto A, Pittaluga S, Vire B, et al. The lymph node microenvironment promotes B-cell receptor signaling, NF-kappaB activation, and tumor proliferation in chronic lymphocytic leukemia. *Blood*. 2011;117:563–74.
41. Suire S, Condliffe AM, Ferguson GJ, Ellson CD, Guillou H, Davidson K, et al. Gbetagammias and the Ras binding domain of p110 $\gamma$  are both important regulators of PI(3)K $\gamma$  signalling in neutrophils. *Nat Cell Biol*. 2006;8:1303–9.
42. Nombela-Arrieta C, Lacalle RA, Montoya MC, Kunisaki Y, Megias D, Marques M, et al. Differential requirements for DOCK2 and phosphoinositide-3-kinase gamma during T and B lymphocyte homing. *Immunity*. 2004;21:429–41.
43. Beltman JB, Maree AFM, de Boer RJ. Analysing immune cell migration. *Nat Rev Immunol*. 2009;9:789–98.
44. Furman RR, Sharman JP, Coutre SE, Cheson BD, Pagel JM, Hillmen P, et al. Idelalisib and rituximab in relapsed chronic lymphocytic leukemia. *N Engl J Med*. 2014;370:997–1007.
45. Dubovsky JA, Chappell DL, Harrington BK, Agrawal K, Andritsos LA, Flynn JM, et al. Lymphocyte cytosolic protein 1 is a chronic lymphocytic leukemia membrane-associated antigen critical to niche homing. *Blood*. 2013;122:3308–16.
46. Fiorcari S, Brown WS, McIntyre BW, Estrov Z, Maffei R, O'Brien S, et al. The PI3-kinase delta inhibitor idelalisib (GS-1101) targets integrin-mediated adhesion of chronic lymphocytic leukemia (CLL) cell to endothelial and marrow stromal cells. *PLoS ONE*. 2013;8:e83830.
47. Okkenhaug K, Bilancio A, Farjot G, Priddle H, Sancho S, Peskett E, et al. Impaired B and T cell antigen receptor signaling in p110 $\delta$  PI 3-kinase mutant mice. *Science*. 2002;297:1031–4.
48. So L, Fruman DA. PI3K signalling in B- and T-lymphocytes: new developments and therapeutic advances. *Biochem J*. 2012;442:465–81.
49. Hirsch E, Katanaev VL, Garlanda C, Azzolino O, Pirola L, Silengo L, et al. Central role for G protein-coupled phosphoinositide 3-kinase gamma in inflammation. *Science*. 2000;287:1049–53.
50. Hannigan M, Zhan L, Li Z, Ai Y, Wu D, Huang CK. Neutrophils lacking phosphoinositide 3-kinase gamma show loss of directionality during N-formyl-Met-Leu-Phe-induced chemotaxis. *Proc Natl Acad Sci USA*. 2002;99:3603–8.
51. Van Haastert PJ, Devreotes PN. Chemotaxis: signalling the way forward. *Nat Rev Mol Cell Biol*. 2004;5:626–34.
52. Shymanets A, Prajwal, Bucher K, Beer-Hammer S, Harteneck C, Numberg B. p87 and p101 subunits are distinct regulators determining class IB phosphoinositide 3-kinase (PI3K) specificity. *J Biol Chem*. 2013;288:31059–68.
53. Brock C, Schaefer M, Reusch HP, Czupalla C, Michalke M, Spicher K, et al. Roles of G beta gamma in membrane recruitment and activation of p110 gamma/p101 phosphoinositide 3-kinase gamma. *J Cell Biol*. 2003;160:89–99.
54. Kurig B, Shymanets A, Bohnacker T, Prajwal, Brock C, Ahmadian MR, et al. Ras is an indispensable coregulator of the class IB phosphoinositide 3-kinase p87/p110gamma. *Proc Natl Acad Sci USA*. 2009;106:20312–7.
55. Rommel C. Taking PI3Kdelta and PI3Kgamma one step ahead: dual active PI3Kdelta/gamma inhibitors for the treatment of immune-mediated inflammatory diseases. *Curr Top Microbiol Immunol*. 2010;346:279–99.
56. Winkler DG, Faia KL, DiNitto JP, Ali JA, White KF, Brophy EE, et al. PI3K-delta and PI3K-gamma inhibition by IPI-145 abrogates immune responses and suppresses activity in auto-immune and inflammatory disease models. *Chem Biol*. 2013;20:1364–74.
57. Brown JR. The PI3K pathway: clinical inhibition in chronic lymphocytic leukemia. *Semin Oncol*. 2016;43:260–4.
58. Jones JA, Robak T, Brown JR, Awan FT, Badoux X, Coutre S, et al. Efficacy and safety of idelalisib in combination with ofatumumab for previously treated chronic lymphocytic leukaemia: an open-label, randomised phase 3 trial. *Lancet Haematol*. 2017;4:e114–26.
59. Gockeritz E, Kerwien S, Baumann M, Wigger M, Vondey V, Neumann L, et al. Efficacy of phosphatidylinositol-3 kinase inhibitors with diverse isoform selectivity profiles for inhibiting the survival of chronic lymphocytic leukemia cells. *Int J Cancer*. 2015;137:2234–42.
60. Balakrishnan K, Peluso M, Fu M, Rosin NY, Burger JA, Wierda WG, et al. The phosphoinositide-3-kinase (PI3K)-delta and gamma inhibitor, IPI-145 (Duvelisib), overcomes signals from the PI3K/AKT/S6 pathway and promotes apoptosis in CLL. *Leukemia*. 2015;29:1811–22.